Chinese Chemical Letters 34 (2023) 108061

Contents lists available at ScienceDirect

Chinese Chemical Letters

journal homepage: www.elsevier.com/locate/cclet

Continuous-flow synthesis and crystal modification of Pigment Red 53

Yuxin Mao[a], Changlu Zhou[a], Chaoying Wang[a], Zhong Xin[a,b,*]

[a] Shanghai Key Laboratory of Multiphase Materials Chemical Engineering, School of Chemical Engineering, East China University of Science and Technology, Shanghai 200237, China
[b] State Key Laboratory of Chemical Engineering, School of Chemical Engineering, East China University of Science and Technology, Shanghai 200237, China

ARTICLE INFO

Article history:
Received 6 September 2022
Revised 9 December 2022
Accepted 12 December 2022
Available online 16 December 2022

Keywords:
C.I. Pigment Red 53
Continuous synthesis
Process optimization
Crystal modification

ABSTRACT

In this study, a continuous-flow procedure containing four steps has been developed to synthesize Pigment Red 53 and modify its crystal structure. This process avoided the problems of conveying highly insoluble reaction intermediates by removing intermediate operating steps. After optimization, the overall yield of Pigment Red 53:1 reached 97.1% in the total residence time of 80 s by this diazotization-coupling-laking-crystal transition process. From batch to continuous flow, the purity of products increased from 97.1% to 98.2% and the median diameter of pigment particles decreased from 14 μm to 1.9 μm. This process achieved a similar crystal transition effect in 18 s as in batch, producing α, δ and ν crystals of Pigment Red 53:2 as expected. In conclusion, this continuous-flow procedure displays advantages in both synthesis and crystal transition, indicating another potential use for industrial application.

Azo lake pigments are water-insoluble precipitation of azo dyes with sulfonate or carboxy groups combining a divalent metal counterion. They present bright color light, good covering power, outstanding light fastness, and stability to acid, alkali and heat. Hence azo lake pigments are widely used in inks, coatings, plastics and other industries [1]. The production process of azo lake pigments is complex, including diazotization, coupling and laking [2]. Usually, surface treatment and crystal transition are also involved. The whole production process consumes time considerably because each reaction takes hours in batch, which results in relatively low production efficiency. Besides, azo lake pigments are manufactured in stirred tanks of over ten cubic meters. Because of the release of substantial azo-coupling reaction heat, fast agitation and slow addition of diazonium salt solutions are necessary to prevent local overheating, increasing energy consumption as well as operating costs [3,4]. Most importantly, inefficient heat transfer and mass transfer in the batches inevitably cause variable local conditions, such as local temperature, local pH and local reactant concentrations. This has a negative effect on the particle size and the particle size distribution, and the color characteristics of pigment products are inconsistent between batches [3]. Therefore, It is necessary to develop processes with intensified mass and heat transfers.

In recent years, with the development of continuous flow technology, the continuous production process is capable of reducing the mass transfer distance, shortening the reaction time, facilitating the control of reaction conditions, thus reducing side reactions and improving both the yield and quality of products [5–13]. As reported in the literature, the synthesis process of dyes and pigments is investigated under continuous flow. Wille *et al.* reported the first successful synthesis of azo pigments in continuous flow, and the mean particle size was significantly reduced from 600 nm to 90 nm compared with those of pigments produced by batch process [14]. Pennemann *et al.* synthesized Pigment Yellow 12 in a semi-continuous process and the glossiness increased by 73% and the transparency by 66% [9]. Wang *et al.* studied the diazotization reaction of red base KD in a continuous-flow system, and the yield of diazonium salt exceeded 99% in only 21.2 s [15]. Wang *et al.* also synthesized Pigment Yellow 14 and the transparency of pigment products synthesized by the continuous flow system increased by 93%–99% [16].

However, problems also exist in continuous flow technology, and a typical one is the blockage while the system contains a large amount of solid [17]. At present, researches on continuous flow mostly take aniline or its derivatives as diazonium components, so that the generated diazonium salt can be dissolved in water [16,18]. Otherwise, organic solvents such as DMF or methanol are used to increase the solubility of insoluble diazonium salts in related researches [19,20]. However, this deviates from the industrialization principle, threatening the economy and safety of the production process and bringing trouble to waste liquid treatment. To

* Corresponding author at: Shanghai Key Laboratory of Multiphase Materials Chemical Engineering, School of Chemical Engineering, East China University of Science and Technology, Shanghai 200237, China.
E-mail address: xzh@ecust.edu.cn (Z. Xin).

https://doi.org/10.1016/j.cclet.2022.108061
1001-8417/

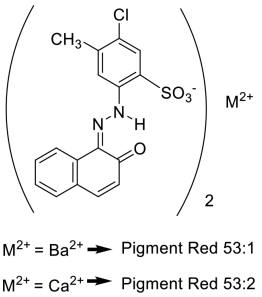

Fig. 1. Pigment Red 53.

deal with this problem, Shukla *et al.* used a bubble column reactor to continuously synthesize Sudan-I dye and Solvent Yellow 16 dye. This continuous process costs almost 4.68 times lower than that of the corresponding batch process and requires 39%–42% less water than the industrial batch process [21].

Pigment Red 53 (P.R.53) is a typical azo red lake pigment, industrially produced in quantities of over 10,000 tons per year with an annual sales volume of several 10 million euros [22]. The diazo component for P.R.53 is 2-amino-4-methyl-5-chlorobenzene sulfonic acid (CLT acid) and the coupling component is 2-naphthol. After the coupling reaction, the sodium salt is treated with $BaCl_2$ to obtain the barium salt P.R.53:1 or $CaCl_2$ to obtain the calcium salt P.R.53:2 (Fig. 1), which is called 'laking' [23]. Then the mixture can be heated in a specific solvent to perform extensive recrystallizations. Due to the poor solubility of reactants, intermediates and products during the synthesis of P.R.53, a large amount of solid is involved in each step of the process. Commonly, continuous diazotization and coupling process are carried out separately, even though they are continuous processes [2,9,18]. Adding intermediate steps between reactions not only reduces the efficiency of production but also increases operating costs. Besides, setting pumps between reactors to power material conveying increases the possibility of back mixing and equipment failure [20]. So it is necessary to investigate this special insoluble system and expand the application of continuous flow in industrial production. Additionally, the above researches only focused on diazotization and coupling reactions. Considering the crystal structure determines the crystal morphology which is related to color strength and dispersion properties, it is valuable to bring laking and crystal transition into the continuous flow and investigate its effect [24,25].

Based on the above considerations, a multi-step continuous integrated production system of the diazotization-coupling-laking-crystal transition process of P.R.53 was established in this work. Taking the yield of P.R.53 as the index, reaction conditions of diazotization and coupling, such as the residence time, temperature and pH were optimized. Then, the effect of sodium nitrite's concentration on the overall yield was investigated. The overall yield of this continuous production system came to 97.1% and the particle size was greatly reduced compared with that of the commercial batch products. The process of crystal transition in continuous flow was also explored and its effect approached that in batch.

Table 1
Reaction conditions of the batch process.

Parameter	Diazotization	Coupling	Laking	Crystal transition
Time (h)	1	1.5	1	2
Temperature (°C)	5	35	35	95
pH	3	8	8	8

The synthetic route and experimental setup of P.R.53:1 were given in Figs. 2 and 3. All the reactants were made into clear solutions and fed by 50 mL syringe pumps or constant-flow pumps [26]. The flow rate of each pump was set at 5 mL/min. The inner diameters of delay loop tubes were 2.5 mm. Tubes were made of PTFE except that for crystal transition, which was made of stainless steel. The reaction time was controlled by the length of the delay loop tube. Ultrasonic vibration was exerted around the diazotization reactor to avoid clogging.

The P.R.53:1 was also synthesized in the batch process for comparison. Reactant solutions were prepared with the same process as Solution A, B, C, D and E. Reaction conditions of the diazotization, coupling, laking and crystal transition process are listed in Table 1. After diazotization, sulfamic acid was introduced to react with the excess sodium nitrite to avoid the generation of nitrous acid.

In this multi-step continuous synthesis system, the flow rate gradually increased in diazotization-coupling-laking-crystal transition reactors as feedings were added. Pumps to feed Solution D and Solution E in Fig. 3 provided extra driving force, preventing coupling and laking reactors from clogging. As soon as the flow in the diazotization reactor remained stable, the whole system could persist for a long time. Ultrasonic vibration exerted around the diazotization reactor was an effective way to realize a stable continuous-flow reaction and the experiments were performed for 10 min without clogging. According to the results of HPLC of the aqueous phase after the multi-step continuous reactions, no dye was detected. It confirmed that all the dyes were turned into laked pigments in the laking reaction. Therefore, reaction conditions of only diazotization and coupling are optimized to increase the overall yield.

The effects of diazotization time (20, 40, 60 s) and temperature (5, 10, 15, 20 °C) on the total yield were investigated. The coupling reaction conditions were fixed at $t = 30$ s, $T = 40$ °C and pH 8. As illustrated in Fig. 4, the highest overall yield reaches 92.1% when the diazotization time is 60 s and the temperature is 5 °C. The yield second to it is 90.8% when the diazotization time is 40 s and the temperature is 10 °C. The yields donot increase with temperature within the same reaction time. The reason for this phenomenon is the thermal instability of diazonium salt. The reaction rate increases with temperature, so the generation and decomposition rate of diazonium salt increases at the same time. When the residence time is 20 s, a lower temperature restricts the diazotization reaction rate and a higher temperature accelerates both the generation and decomposition rate of the diazonium salt. Therefore, the yield was kept at a relatively low level. When the residence time is 40 s, the decomposition of diazonium salt significantly reduces the yield when the temperature increases from 10 °C to 15 °C. At

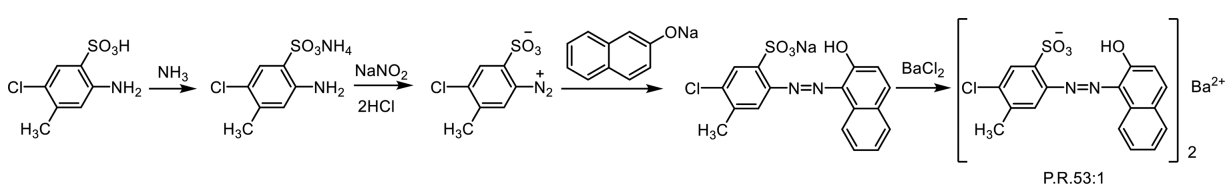

Fig. 2. Continuous-flow synthesis of P.R.53:1.

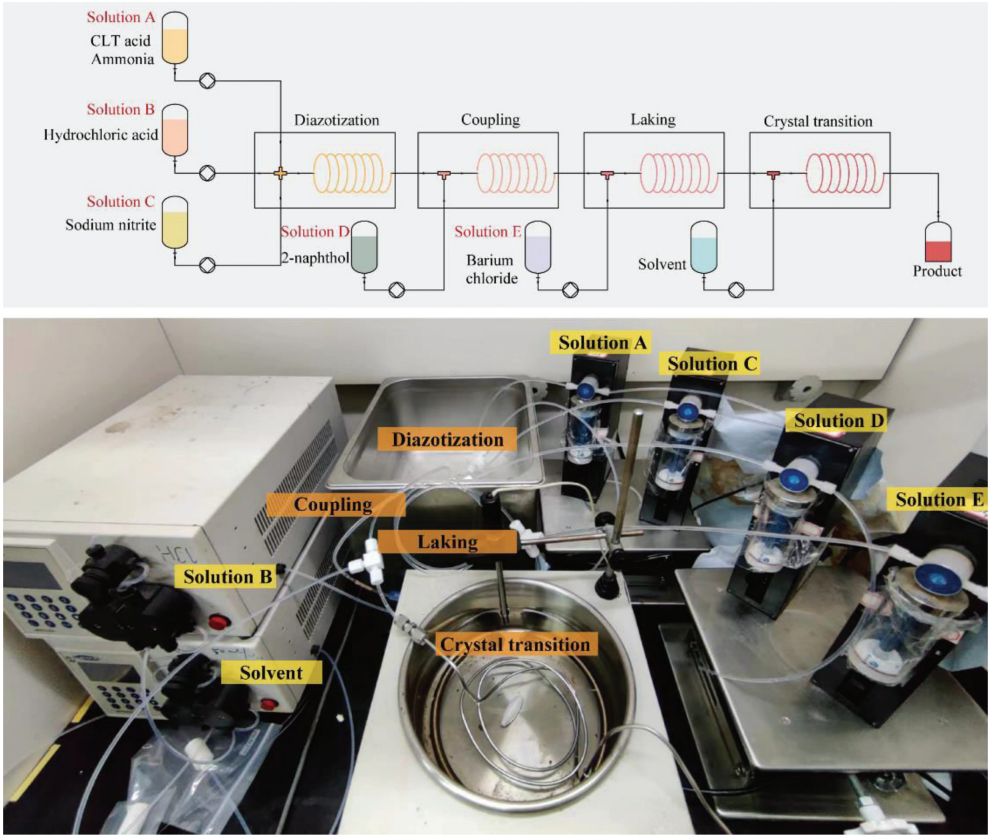

Fig. 3. Experimental setup for the continuous-flow synthesis of P.R.53:1.

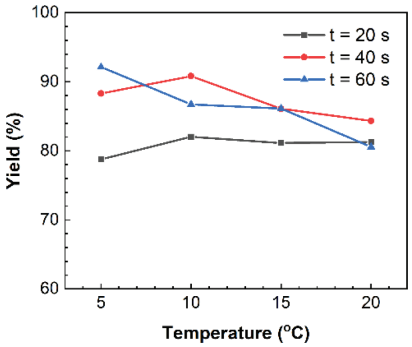

Fig. 4. Effects of diazotization conditions on the overall yield of the system.

the residence time of 60 s, lower temperature effectively restrained the decomposition of diazonium salt and the long residence time ensured the accomplishment of the diazotization reaction, so the yield decreased with temperature. To strike a balance between the yield and the energy consumption, the diazotization reaction was carried out at the residence time of 40 s and the temperature of 10 °C.

According to the previous studies [15,16], reaction time, temperature and pH would affect the yield of the coupling reaction. To explore the influence of these parameters on the coupling reaction, the orthogonal experiment of three factors at three levels was designed and the results were shown in Table 2.

As shown in Table 3, the relative size of the range (R) indicates the extent of influence: Factor C > Factor B > Factor A. Apparently coupling pH is the main factor affecting the yield of the coupling reaction and the reaction temperature is the secondary factor. The coupling reaction rate decreases at higher pH because the diazonium ion turns into diazotate ion [27]. As the reaction temperature increases, part of the diazonium salt decomposes before participating in the coupling reaction. The residence time of the coupling reaction has little effect on the yield. This means the coupling reaction is a fast reaction and a short time is enough for it to finish. After the orthogonal test, the optimal conditions by calculation were determined as $t = 10$ s, $T = 40$ °C and pH 7.5. The overall yield was 93.5% under these optimal conditions and the stability of the result was verified by three repeated experiments. Other parameters are shown in Table 4.

Apart from the optimization of the diazotization and coupling conditions, the amount of sodium nitrite also needed discussion. Excessive sodium nitrite among acid diazonium salt existed in the form of nitrous acid, which has an adverse effect on the coupling reaction [18]. In this multi-step continuous production system, excessive sodium nitrite is not removed by intermediate steps. Therefore, the molar ratio of sodium nitrite to diazo component should be as close as possible to 1:1. However, a lower sodium nitrite concentration will reduce the diazotization reaction rate. Based on the above considerations, the effect of different sodium nitrite ratios on the total yield of the reaction was explored. As shown in Fig. 5, the highest overall yield was found to be 97.1% when the molar ratio of sodium nitrite to diazo component was 1.05. When the amount of sodium nitrite was close to that of diazo component, the effect of sodium nitrite concentration on the increase of diazotization reaction rate could be ignored, and the adverse effect of excess sodium nitrite played a prominent role.

This diazotization-coupling-laking-crystal transition process was carried out in both continuous flow and batch to verify the advantage of continuous flow. The purity of P.R.53:1 synthesized in continuous flow was found to be 98.2%, whereas the pigment product synthesized in batch had a purity of 97.1%. The improvement in purity is owing to the superior mass and heat transfer

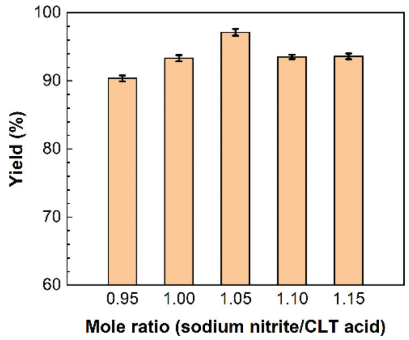

Fig. 5. Overall yield of reaction under different ratios of sodium nitrite.

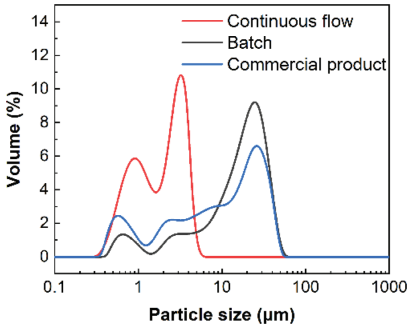

Fig. 6. Particle size distribution of P.R.53:1 synthesized in batch and continuous flow.

characteristics of the continuous-flow system. Because of the solubility in aqueous solutions, most of the diazonium salts exist in the solid form. We have concluded that the coupling is a rather fast reaction from the above experiments, so the formed dyes particles precipitate quickly from the medium and some of them may deposit on the surface of unreacted diazonium salts. The continuous-flow process enables instant mixing and reduces the mass transfer distance, partly alleviating the above problem and increasing the purity of the product.

The advantages of mass and heat transportation in continuous-flow synthesis can also explain the improvement in particle size distribution. For comparison, the particle size of commercial P.R.53:1 (Shanghai Macklin Biochemical Technology Co., Ltd.) was also tested. As shown in Fig. 6, the continuous-flow process reduced the particle size greatly and narrowed the particle size distribution range. The product synthesized in continuous flow has a median diameter $d(0.5)$ of 1.9 μm, which is far smaller than that of the product synthesized in batch (14 μm). The two peaks in the particle size distribution come from the further processing steps. Filtration and drying lead to particle agglomeration and bonding. It is difficult for these extremely tiny particles to redisperse in the dispersant water after agglomeration, so the particle size distribution deviates from the normal distribution.

To further discuss the role of continuous flow in the synthesis of azo pigments, the effect of continuous-flow crystal transition was explored. The properties of pigment products depend on the solid-state structure of the pigments. Being heated in appropriate solvents, α crystals are transformed into other stable crystals with regular arrangement after dissolution and recrystallization [28]. Comparing X-ray powder diffraction data of materials with that of known structure, the crystal form can be qualitatively identified [29–32]. However, the low solubility of pigments makes it difficult to prepare single crystals, impeding the acquirement of X-ray powder diffraction data [33]. Therefore, the diffraction angle

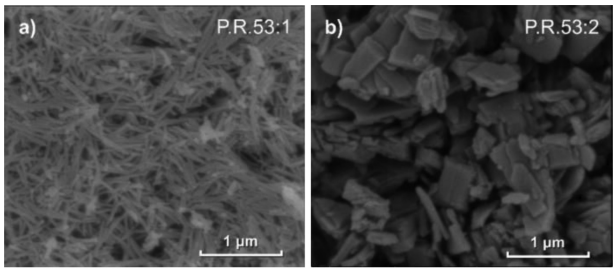

Fig. 7. Particle morphology of SEM: (a) P.R.53:1; (b) P.R.53:2.

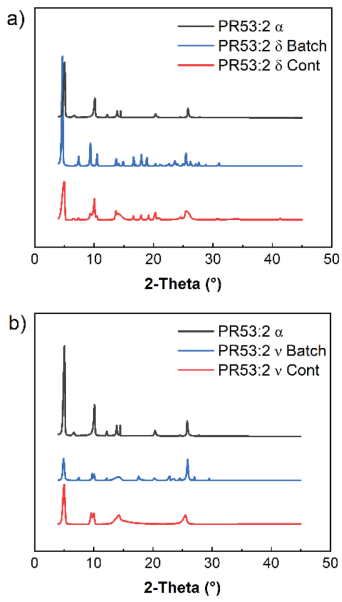

Fig. 8. XRD diffraction patterns of P.R.53:2 prepared in continuous flow and batch with different solvents: (a) δ crystals, solvent: chlorobenzene; (b) ν crystals, solvent: ethylene glycol.

of the main diffraction peaks was compared with that in literature to determine the crystal form of the prepared pigment [34–36].

Through SEM test, it was found that the particle morphology of P.R.53:1 was different from that of P.R.53:2. As shown in Fig. 7, the former exhibited a long strip shape and the latter was in a sheet shape. Therefore, the SEM diffraction pattern of P.R.53:2 shows more significant crystal characteristics. So P.R.53:2 was selected as the subject to study crystal modification.

Firstly, P.R.53:2 of different crystal forms were prepared in batch. After filtration, the P.R.53:2 product of α crystals was heated in chlorobenzene and ethylene glycol under reflux for 2 h to obtain δ and ν crystals separately. After that, it was filtered, washed with the same solvent and dried at 100 °C for 12 h. Following the process in Fig. 2, these solvents were introduced into the crystallization process to prepare different crystals continuously. The residence time in the crystal transition process was controlled at 18 s and the temperature was 100 °C. The XRD diffraction peaks of the products synthesized in continuous flow and batch are shown in Fig. 8 for comparison and the diffraction angles of the characteristic peaks are listed in Tables S1–S5 (Supporting information). There are marked similarities between the P.R.53:2 crystallized in continuous flow and batch. For instance, after being heated in chlorobenzene, pigment product synthesized in continuous flow exhibited characteristic peaks of δ crystals at the diffraction angle with the diffraction intensity of 4.6°(80.9), 9.4°(16), 10.5°(9.8), 16.7°(10.6), 25.4°(15.2). However, characteristic peaks of α crystals, such as at the diffraction angle of 5.1°(100), 10.0°(41.3), 13.7°(16.6),

Table 2
The results of orthogonal test for the coupling reaction.

No.	Factor A Time (s)	Factor B Temp (°C)	Factor C pH	Yield (%)
1	10	30	7.5	90.5
2	10	40	8.5	89.9
3	10	50	9.5	78.0
4	20	30	9.5	85.1
5	20	40	7.5	81.9
6	20	50	8.5	88.7
7	30	30	8.5	75.5
8	30	40	9.5	90.4
9	30	50	7.5	89.3

Table 3
Range analysis for the coupling reaction.

No.	Factor A Time (s)	Factor B Temp (°C)	Factor C pH
k1 (%)	86.1	83.7	89.9
k2 (%)	85.2	87.4	88.1
k3 (%)	85.1	85.3	78.5
R	1.1	3.7	11.4
Optimum group	A_1	B_2	C_1

k: the average value of each level of each factor.
R: the difference between the average values of the factors.

Table 4
Process conditions in synthesis of P.R.53:1.

Conditions	Diazotization	Coupling	Laking	Crystal transition
Residence time (s)	40	10	12	18
Liquid holdup (mL)	10.0	3.3	5.0	7.4
Coil length (cm)	204	68	102	150
Temperature (°C)	10	40	30	80

14.4°(11.1), 20.4°(17), are also presented, which means the crystal transition was not completed to the full extent due to the limited crystal transition time and solubility in the solvents. As shown in Fig. 8b, the characteristic peaks of the ν crystals synthesized in continuous flow appear at the diffraction angle of 9.7°(30.5), 10.2°(30.5), 25.0°(18.7), 25.2°(9.1). To explore the effects of crystal transition temperature, the same procedures were carried out at 60 °C and 80 °C separately and the crystals showed no signs of δ or ν crystals. Temperatures higher than 100 °C would generate a large amount of vapor, thus causing instability in the system with pumps. So the transition temperature is supposed to be fixed at 100 °C in favor of the crystal transition effect.

In this work, a multi-step continuous integrated production system of the diazotization-coupling-laking-crystal transition process of azo lake pigments was established. This continuous-flow process helps to avoid the problems in conveying highly insoluble reaction intermediates. After the optimization of process parameters, the overall yield of the diazotization-coupling-laking-crystal transition process for the synthesis of Pigment Red 53:1 reached 97.1% in the total residence time of 80 s. From batch to continuous flow, the purity increased from 97.1% to 98.2% and the median diameter of pigment particles decreased from 14 μm to 1.9 μm. Furthermore, this continuous-flow process achieved a similar crystal transition effect as in batch, producing α, δ and ν crystals of Pigment Red 53:2 as expected.

Declaration of competing interest

The authors declare that they have no known competing financial interests or personal relationships that could have appeared to influence the work reported in this paper.

Acknowledgments

The authors would like to acknowledge financial support from Shanghai Municipal Science and Technology Commission (No. 21520761100), the Open Project of State Key Laboratory of Chemical Engineering (No. SKL-ChE-21C07), and the Fundamental Research Funds for the Central Universities, and the Program of Leading Talents (2013).

Supplementary materials

Supplementary material associated with this article can be found, in the online version, at doi:10.1016/j.cclet.2022.108061.

References

[1] K. Hunger, P. Mischke, W. Rieper, Ullmann's Encyclopedia of Industrial Chemistry, 5th. ed., Wiley-VCH, Weinheim, 2017.
[2] U. Nickel, K. Kund, F. Alfter, JP: JP2001–184775, 2002.
[3] I. Szele, H. Zollinger, Preparative Organic Chemistry, Springer, Berlin Heidelberg, 1983.
[4] Z. Shi, X. Wang, D. Yin, Org. Process Res. Dev. 26 (2021) 661–669.
[5] M. Köckinger, B. Wyler, C. Aellig, Org. Process Res. Dev. 24 (2020) 2217–2227.
[6] N. Kockmann, M. Gottsponer, D.M. Roberge, Chem. Eng. J. 167 (2011) 718–726.
[7] S.J. Miller, H. Ishitani, Y. Furiya, Org. Process Res. Dev. 25 (2021) 192–198.
[8] F.M. Akwi, P. Watts, Chem. Commun. 54 (2018) 13894–13928.
[9] H. Pennemann, S. Forster, J. Kinkel, Org. Process Res. Dev. 9 (2005) 188–192.
[10] Z.Q. Yu, G. Tong, X.X. Xie, Org. Process Res. Dev. 19 (2015) 892–896.
[11] Z.Q. Yu, X.X. Xie, H. Dong, Org. Process Res. Dev. 20 (2016) 774–779.
[12] J. Ren, M. Wu, K. Dong, Chin. Chem. Lett. 34 (2023) 107694.
[13] Y. Xin, S. Peng, J. Chen, Chin. Chem. Lett. 31 (2020) 1448–1461.
[14] C. Wille, H.P. Gabski, T. Haller, Chem. Eng. J. 101 (2004) 179–185.
[15] F.J. Wang, A. Chen, S.D. Ling, React. Chem. Eng. 6 (2021) 1462–1474.
[16] F.J. Wang, J.P. Huang, J.H. Xu, Org. Process Res. Dev. 23 (2019) 2637–2646.
[17] A. Pomberger, Y.M. Mo, K.Y. Nandiwale, Org. Process Res. Dev. 23 (2019) 2699–2706.
[18] F.J. Wang, Y.C. Ding, J.H. Xu, Ind. Eng. Chem. Res. 58 (2019) 16338–16347.
[19] F.M. Akwi, P. Watts, Beilstein J. Org. Chem. 12 (2016) 1987–2004.
[20] F.J. Wang, J.P. Huang, J.H. Xu, Chem. Eng. Process 127 (2018) 43–49.
[21] C.A. Shukla, M.S. Kute, A.A. Kulkarni, Green Chem. 23 (2021) 6614–6624.
[22] W. Herbst, K. Hunger, G. Wilker, Industrial Organic Pigments (Production, Properties, Applications), 3rd ed., Wiley-VCH, Weinheim, 2004.
[23] T. Gorelik, M.U. Schmidt, J. Bruning, Cryst. Growth Des. 9 (2009) 3898–3903.
[24] A.R. Kennedy, C. Mcnair, W.E. Smith, Angew. Chem. Int. Edit. 39 (2000) 638.
[25] W. Luo, F. Liu, Y. Guo, Chin. Chem. Lett. 34 (2023) 107636.
[26] Y. Mao, Z. Xin, CP: CN202210876093.9, 2022.
[27] R. Kaminski, U. Lauk, P. Skrabal, Helv. Chim. Acta 66 (1983) 2002–2017.
[28] J. Schröder, Prog. Org. Coat. 16 (1988) 3–17.
[29] L. Tapmeyer, D. Eisenbeil, M. Bolte, Acta Crystallogr. E Crystallogr. Commun. 77 (2021) 402–405.
[30] L. Tapmeyer, S. Hill, M. Bolte, Acta Crystallogr. C: Struct. Chem. 76 (2020) 716–722.
[31] S.N. Ivashevskaya, J. Van De Streek, J.E. Djanhan, Acta Crystallogr. B: Struct. Sci. 65 (2009) 212–222.
[32] E.A. Kabova, J.C. Cole, O. Korb, J. Appl. Crystallogr. 50 (2017) 1421–1427.
[33] S.N. Ivashevskaya, Acta Crystallogr. E Crystallogr. Commun. 73 (2017) 507–510.
[34] M.U. Schmidt, EP: EP99110831. 7, 2002.
[35] S.M.U. Dr., M.H.J. Dr, EP: EP0965616, 1999.
[36] F. Schui, R. Deubel, N. Wester, Canada Patent: CA1219858 A1, 1987.